Mössbauer-Effect Determination of the Crystalline Electric Field Parameters in Thulium Metal*

D. L. Uhrich† and R. G. Barnes
Institute for Atomic Research and Department of Physics, Iowa State University, Ames, Iowa

(Received 8 June 1967)

By measuring the temperature dependence of the nuclear quadrupole splitting of the 8.42-keV Mössbauer transition in the paramagnetic state of thulium metal, a determination of the crystalline electric field (CEF) parameters of elemental thulium has been obtained. The nuclear quadrupole interaction was studied within the temperature range 59 to 156°K. It was found that a zero-order calculation was sufficient to fit theory to experiment, and that in particular only C_2^0, ρ_1, and ρ_2' (where the ρ's account for shielding constants and the temperature-independent contributions to the electric field graident at the nucleus) were needed to fit the theory to the data. The remaining CEF parameters, C_4^0, C_6^0, and C_6^6, were constrained to equal zero in the fitting routine. The over-all splitting of the $^3H_6$ ground multiplet was found to be 76.1 cm^{-1}. This study also includes a determination of electronic shielding factors for thulium. The atomic Sternheimer factor R_Q was found to be 0.16; and the constant σ_2, which represents the shielding of the $4f$ shell from the CEF by the closed outer shells, was found to be 0.34. The latter quantity was obtained under the assumption that screening of the Tm^{+3} ions by the conduction electrons can be neglected. The direct lattice contribution and the conduction-electron contribution to the net electric field gradient at the Tm nucleus were found to be positive and of the same order of magnitude.

I. INTRODUCTION

RECENTLY, the technique of recoil-free resonance spectroscopy was applied by Mössbauer and coworkers to the study of the crystalline electric field (CEF) interaction in thulium salts.[1] In a paramagnetic solid, the first excited nuclear level of Tm^{169} is split by the interaction of the electric quadrupole moment of that level with the electric field gradient (EFG) at the nuclear site. The EFG at the nucleus results in general from the combination of an essentially temperature-independent lattice contribution and a strongly temperature-dependent contribution from the $(4f)^{12}$ electronic configuration of the ion itself. The latter contribution reflects directly the interaction of the CEF potential with the $4f$-electron cloud so that the measurement of the temperature dependence of the quadrupole interaction strength can be employed to evaluate the CEF parameters.

The importance of CEF effects in ferromagnetic, antiferromagnetic, and ferrimagnetic materials has long been recognized. In metals, the exchange interaction which leads to magnetic ordering usually dominates the CEF interaction, and the principal effect of the latter is to set up an anisotropy energy.[2] Rare-earth salts, however, lie at the opposite extreme where the exchange interaction is weak compared with CEF effects. Finally, intermetallic compounds afford examples in which the two interactions are often of comparable magnitude.

No direct and easy method exists for determining the CEF parameters and the magnitude of the energy splitting Δ of the $(4f)^n$ ground state in the rare-earth metals. By using a two-parameter molecular-field model to fit the magnetic specific-heat anomaly and the bulk susceptibility data, Bleaney was able to determine the CEF parameters and Δ in praseodymium metal.[3] Two attempts have been made to estimate Δ for cubic cerium metal. From magnetic-susceptibility and specific-heat measurements, Murao and Matsubara[4] calculated $\Delta=206$–240°K while Rainford[5] found $\Delta=135\pm35$°K on the basis of neutron-scattering experiments. No measurements of this sort appear to have been made on any of the heavy rare earths.

Thulium metal affords a unique opportunity to measure these quantities by utilizing the Mössbauer effect. Since the magnetic ordering temperature of thulium is relatively low (56°K, the lowest of the heavy rare earths), and since the Mössbauer γ-transition energy is only 8.42 keV and the relevant nucleus (Tm^{169}) is 100% abundant, the CEF effects may be easily and directly observed via the quadrupole splitting of the Mössbauer γ-transition. That such a splitting is observed is a consequence of the hexagonal (D_{6h}) crystal symmetry which provides an axially symmetric EFG which splits the nuclear excited state ($I=\frac{3}{2}$).

Previous Mössbauer-effect studies of thulium metal have been limited in the main to the magnetically ordered regions below the Néel temperature of 56°K. The only exception, apart from room-temperature data, is a single determination by Kalvius *et al.*, of the quadrupole splitting at 60°K.[6] We have repeated that measurement and have made further measurements at

* Work was performed in the Ames Laboratory of the U.S. Atomic Energy Commission. Contribution No. 2102.
† Present address: Kent State University, Kent, Ohio.
[1] R. G. Barnes, R. L. Mössbauer, E. Kankeleit, and J. M. Poindexter, Phys. Rev. **136**, A175 (1964).
[2] R. J. Elliott, Phys. Rev. **124**, 346 (1961).
[3] B. Bleaney, Proc. Roy. Soc. (London) **276**, 39 (1963).
[4] T. Murao and T. Matsubara, Progr. Theoret. Phys. (Kyoto) **18**, 215 (1957).
[5] B. D. Rainford, in Rare Earth Research Conference, Durham, England, 1966 (unpublished).
[6] M. Kalvius, P. Kienle, H. Eicher, W. Wiedemann, and S. Schüler, Z. Physik **172**, 231 (1963).

roughly 5 to 10°K intervals up to 170°K. The CEF parameters and Δ have been evaluated from this temperature dependence. A preliminary report of the work has been given elsewhere.[7]

In the following, we first recapitulate briefly the relevant theory for the temperature dependence of the quadrupole splitting of a rare-earth nucleus. The experimental results are presented following a resume of the experimental details and the numerical analysis. Finally, the CEF parameters and Δ are discussed and compared with various estimates of these quantities.

II. THEORY

For the case of nonmetallic salts of thulium, the application of standard CEF theory to the temperature dependence of the quadrupole splitting of the Tm^{169} Mössbauer line has been treated in detail in Ref. 1. Our interpretation of the corresponding splitting in metallic substances follows closely that treatment, and as nearly as possible, we shall employ the notation of Ref. 1.

In optically transparent substances, the first excited level $^3H_4$ of the ground spin-orbit multiplet of the Tm^{3+} ion lies some 5600 cm^{-1} above the ground level $^3H_6$, so that this and other higher levels may be neglected in calculating the behavior of quantities in the temperature range up to at least 300°K. We shall assume that in the metallic case these higher optical levels may also be neglected insofar as the interpretation of temperature-dependent properties below 200°K is concerned.

Thulium metal is hexagonal close packed so that the point symmetry at the nuclear site is D_{6h}. The quadrupole coupling is determined entirely by the axial (z) component of the EFG tensor. We begin by writing for this component

$$eq_{zz}=(1-\gamma_\infty)\,eq_{zz}^{(\mathrm{lat})}+(1-R_Q)\,eq_{zz}^{(4f)}+eq_{zz}^{(\mathrm{ce})}, \quad (1)$$

which is Eq. (10) of Ref. 1, augmented by the final term which represents the contribution due to the non-s character of the conduction electrons. The Sternheimer antishielding and shielding factors γ_∞ and R_Q, respectively, take account of the contributions which closed electron shells make to the EFG arising from the lattice of point charges and from the partially filled $4f$ shell. As in the case of thulium salts, we assume that the temperature dependence of the EFG is due entirely to the temperature dependence of the $4f$-electron contribution, $(1-R_Q)eq_{zz}^{(4f)}$, so that we have for the temperature dependence of q_{zz},

$$\langle q_{zz}\rangle_T=(1-\gamma_\infty)\,q_{zz}^{(\mathrm{lat})}+(1-R_Q)\,\langle q_{zz}^{(4f)}\rangle_T+q_{zz}^{(\mathrm{ce})}, \quad (2)$$

with

$$\langle q_{zz}^{(4f)}\rangle_T = \sum_{\nu=1}^{2J+1}\langle\nu\,|\,q_{zz}^{(4f)}\,|\,\nu\rangle\exp(-E_\nu/kT)\Big/\sum_{\nu=1}^{2J+1}\exp(-E_\nu/kt). \quad (3)$$

Here, the energies E_ν and wave functions $|\nu\rangle$ of the individual CEF levels are determined by diagonalization of the Hamiltonian which describes the interaction of the CEF with the electrons of the partially filled $4f$ shell, using as basis functions the $2J+1$ degenerate functions belonging to the electronic ground state of the $4f$ configuration which is characterized by total angular momentum J ($J=6$ for Tm^{3+}). That Hamiltonian is Eq. (3) of Ref. 1,

$$\mathfrak{H}_{\mathrm{CEF}}^{(4f)}=\sum_k\sum_{n,m}A_n^m[r_k^n+S_n(r_k)]\Phi_n^m(\theta_k,\phi_k) \quad (4)$$

and the relevant matrix elements are

$$\mathfrak{H}_{m_J,m_J'}=\sum_{n,m}A_n^m\langle r^n\rangle_E\langle J\,||\,\theta_n\,||\,J\rangle \times\langle J,m_J\,|\,O_n^m(J_x,J_y,J_z)\,|\,J,m_J'\rangle, \quad (5)$$

where

$$\langle r^n\rangle_E=(1-\sigma_n)\,\langle r^n\rangle_{4f},$$
$$\sigma_n=\langle U_{4f}\,|\,S_n(r)\,|\,U_{4f}\rangle/\langle r^n\rangle_{4f},$$
$$\langle r^n\rangle_{4f}=\langle U_{4f}\,|\,r^n\,|\,U_{4f}\rangle.$$

In these expressions, U_{4f} is the radial part of the electronic wave functions for the $4f$ shell. The functions $O_n^m(J_x,J_y,J_z)$ are operator equivalents; those relevant to the present work are tabulated in the literature.[8] The expressions $\langle J\,||\,\theta_n\,||\,J\rangle$, $n=2$, 4, 6, are reduced matrix elements which are also tabulated in the literature.[8] The A_n^m represent lattice sums over point charges and effective multipole moments in the surrounding ions.

The factors σ_n are shielding parameters which represent to a first approximation the shielding of the $4f$ electrons from the CEF by the outer $5s^25p^6$ shells of the rare-earth ion. This shielding has been shown to be important for the C_2^0 CEF parameter, whereas for the other terms, C_n^m [where $C_n^m=A_n^m\langle r^n\rangle_{4f}(1-\sigma_n)$], with $n>2$, shielding contributes a negligible effect. The relation between the theoretical (nonshielded) product of the lattice sum A_2^0 and the radial average $\langle r^2\rangle_{4f}$, $A_2^0\langle r^2\rangle_{4f}$, and the experimentally determined CEF parameter C_2^0 is given by

$$C_2^0=A_2^0\langle r^2\rangle_E=A_2^0(1-\sigma_2)\,\langle r^2\rangle_{4f}. \quad (6)$$

In their work on the rare-earth trichlorides, Lenander and Wong concluded that "huge" shielding of A_2^0 oc-

[7] D. L. Uhrich, D. J. Genin, and R. G. Barnes, Phys. Letters **24A**, 338 (1967).

[8] W. Low, in *Solid State Physics*, edited by F. Seitz and D. Turnbull (Academic Press Inc., New York, 1960), Suppl. 2.

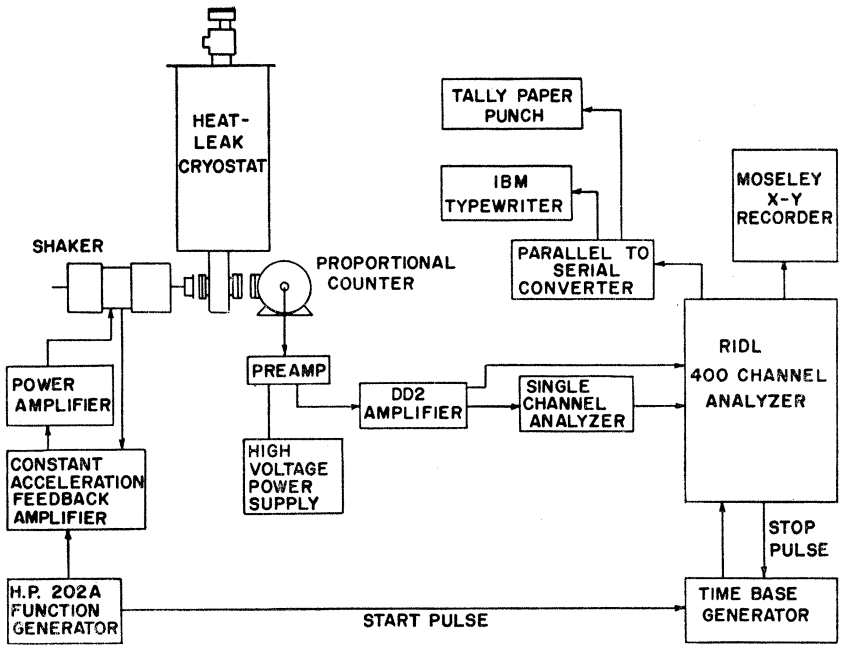

FIG. 1. Block diagram of the Mössbauer-effect spectrometer. The source oven was located on the end of the shaker nearest the cryostat, and the absorber in the tail of the cryostat.

curred.[9] Calculations of σ_2 for Tm^{3+} ions vary from 0.1 to 0.59,[10] with the most recent calculation by Sternheimer giving $\sigma_2=0.48$.[11]

The various separate contributions to the net temperature-dependent EFG at the nucleus, $\langle q_{zz}\rangle_T$, are given by

$$e^2q_{zz}^{(\mathrm{lat})}=-4A_2^0, \tag{7}$$

$$\langle v\mid q_{zz}^{(4f)}\mid v\rangle=-\langle J\mid\mid\theta_2\mid\mid J\rangle\langle r^{-3}\rangle_{4f}\langle v\mid 3J_z^2-J^2\mid v\rangle, \tag{8}$$

and

$$q_{zz}^{(\mathrm{ce})}=Z\langle\phi\mid(3z^2-r^2)r^{-5}\mid\phi\rangle, \tag{9}$$

where in the last expression $\mid\phi\rangle$ represents all of the conduction electrons, not just those at the Fermi surface. Z is the number of conduction electrons per ion.

Since the ground-state spin of Tm^{169} is $\frac{1}{2}$ and the excited-state spin is $\frac{3}{2}$, the quadrupole splitting is due entirely to the excited state and is given by just half the coupling constant so that this directly measured quantity is given by

$$\langle\Delta E\rangle_T=\tfrac{1}{2}e^2Q\langle q_{zz}\rangle_T. \tag{10}$$

This equation may be written in detail by combining Eqs. (2), (3), and (6)–(9) to yield

$$\langle\Delta E\rangle_T=\tfrac{1}{2}e^2Q[\langle J\mid\mid\theta_2\mid\mid J\rangle\langle r^{-3}\rangle_{4f}(1-R_Q)\langle 3J_z^2-J^2\rangle_T+4C_2^0(1-\gamma_\infty)/e^2\langle r^2\rangle_E-q_{zz}^{(\mathrm{ce})}]. \tag{11}$$

Here $\langle 3J_z^2-J^2\rangle_T$ is the thermal average of $3J_z^2-J^2$ evaluated in the same fashion as that for $q_{zz}^{(4f)}$ in Eq. (3). Direct comparison of the experimental results with theory within the framework of the CEF model is facilitated by replacing all quantities in this last expression which involve radial integrals by experimentally determinable parameters. The nuclear quadrupole moment is treated in similar fashion. We introduce the dimensionless parameters

$$\rho_1=e^2Q\langle r^{-3}\rangle_{4f}(1-R_Q)\langle J\mid\mid\theta_2\mid\mid J\rangle/C_2^0, \tag{12}$$

$$\rho_2'=\frac{Q(1-\gamma_\infty)}{\langle r^2\rangle_{4f}(1-\sigma_2)}-\frac{e^2q_{zz}^{(\mathrm{ce})}Q}{4C_2^0} \tag{13}$$

to be determined from the experimental data. The prime is used on ρ_2' to distinguish it from a similar parameter introduced in Ref. 1 but which did not include a conduction-electron contribution to the EFG. Written in terms of these parameters, the quadrupole splitting becomes

$$\langle\Delta E\rangle_T=\tfrac{1}{2}C_2^0[\rho_1\langle 3J_z^2-J^2\rangle_T+4\rho_2']. \tag{14}$$

In the present situation, dealing with a metal, we do not have experimentally (e.g., optically) determined CEF parameters available, and in fact, the elucidation of these parameters from the temperature dependence of the quadrupole splitting is the major goal of this work. In order to make a start at analyzing the quadrupole splitting behavior, initial estimates of the CEF parameters are required. We shall base these estimates on numerical calculation of the lattice sums A_n^m, theoretical values for the radial integrals, the empirical value of the shielding parameter σ_2, and an estimate of the splitting parameter Δ obtained from the tem-

[9] C. J. Lenander and E. Y. Wong, J. Chem. Phys. **38**, 2750 (1963).
[10] G. Burns, Phys. Rev. **128**, 2121 (1962); D. K. Ray, Proc. Phys. Soc. (London) **82**, 47 (1963); R. E. Watson and A. J. Freeman, Phys. Rev. **133**, A1571 (1964); M. N. Ghatikar, A. K. Raychaudhuri, and D. K. Ray, Proc. Phys. Soc. (London) **86**, 1235 (1965).
[11] R. M. Sternheimer, Phys. Rev. **146**, 140 (1967).

perature at which the quadrupole splitting effectively disappears.

III. EXPERIMENTAL DETAILS

A. Spectrometer System

The Mössbauer spectrometer (Fig. 1) employed in this work is of conventional construction, the design of Kankeleit[12] being used for the transducer, with a constant-acceleration feedback amplifier modeled after the one developed by Cohen *et al.*[13] The drive system was normally operated at a frequency of 12 cps. Velocities up to ± 16 cm/sec were readily attained. A proportional counter, similar to those constructed at the California Institute of Technology, was used to detect the 8.42-keV radiation.[14]

Calibration of the spectrometer drive was performed using the Mössbauer-effect spectrum of Armco iron. The successful utilization of the relatively small velocity splitting of the iron spectrum as a calibration for the twenty times larger velocities required by the thulium spectra requires that the response of the drive electronics be linear over this range. Iron calibrations based on different full-scan velocity settings were found to be internally consistent to better than 2%. Also, measurements of the quadrupole splitting in Tm_2O_3 at 77 and 300°K were in excellent agreement with the values previously obtained using a constant-velocity drive unit.

The various absorber temperatures were obtained by using a heat-leak cryostat. Helium, hydrogen, or nitrogen could be used in the inner Dewar of the cryostat, and the outer nitrogen Dewar was automatically refilled every 4 h during operating periods. A temperature control designed and built by co-workers maintained the temperature setting within ± 0.5°K over the range 4.2–300°K.

The sample chamber within the cryostat was accessible from the top to permit changing absorbers while the cryostat was cold. The absorber, attached to a copper holder, could be lowered into or fished out of the sample chamber by means of a threaded thin stainless rod. The flat absorbers were aligned perpendicular to the γ-ray beam by a slot in the sample chamber. Four 0.020-in. Be and two 0.001-in. Mylar windows in the path of the radiation resulted in a net transmission of the cryostat for the 8.42-keV radiation of only about 10%.

B. Absorbers and Sources

The thulium metal absorber was prepared by rolling a button of the metal into a foil of thickness 0.001 in. (0.025 mm). A series of anneals (at 775°C) were needed as the metal work-hardened in the rolling process. The final foil was then polished and annealed. Comparison of spectra showed, however, that this last step had no effect on the data.

TABLE I. Comparison of linewidths of the Tm^{169} Mössbauer resonance in Tm metal at room temperature. All absorbers were in the form of rolled foils.[a]

Source	Absorber thickness (10^{-3} in.)	Linewidth (cm/sec)
$Er_{0.1}Al_{0.9}$ (wt %)	0.5[b]	2.9
$Er_{0.1}Al_{0.9}$ (wt %)	0.8	3.4
Er_2O_3 (at 400°C)	0.8	4.0
$Er_{0.1}Al_{0.9}$ (at. %)	1.0[b]	3.0

[a] 10^{-3}-in. foil of Tm metal = 23.2 mg of Tm/cm².
[b] Annealed at 775°C for 2 h.

All of the data were initially obtained by using a source of neutron-irradiated Er_2O_3 which was maintained at 400°C to ensure a single-line source spectrum. Subsequently, a sampling of the spectra was remeasured using a room-temperature source of $Er_{0.1}Al_{0.9}$, which provides a narrower source line and hence somewhat better resolution.[15] This material offers the considerable practical advantage that the source does not need to be maintained at an elevated temperature as is the case with either the oxide or fluoride. From the phase diagram of the Er-Al system, it appears that this alloy consists of the intermetallic compound $ErAl_3$ dispersed in an aluminum matrix. In $ErAl_3$ the Er occupies a site of cubic symmetry so that no quadrupole splitting of the source line occurs. The low-temperature splittings measured in the metal were independent of the source material.

Table I lists the linewidth as a function of thickness for three room-temperature metal absorbers. Also, in one case, a comparison is given of the linewidth data for one of the metal absorbers obtained using both oxide and alloy sources.

A Mössbauer transmission spectrum of two distinct lines was observable from 59–121°K. From 130–156°K one line whose width decreased with temperature was observed. This broad line could be fitted with two Lorentzian lines whose separation decreased as the temperature increased. The resultant splittings were consistent with the resolved data as is clear from Fig. 3. Above 156°K one line whose width was independent of temperature was observed. Points were taken at 174, 201, 243, and 296°K with the oxide source. All of these lines had the same width (3.8 cm/sec) within the experimental uncertainty.

IV. ANALYSIS

The data analysis, to be described, was performed on an IBM 360/50 computer. In order to eliminate

[12] E. Kankeleit, Rev. Sci. Instr. **35**, 194 (1964).
[13] R. L. Cohen, P. G. McMullin, and G. K. Wertheim, Rev. Sci. Instr. **34**, 671 (1963).
[14] J. M. Poindexter, Ph.D. thesis, Department of Physics, California Institute of Technology, Pasadena, 1964 (unpublished).
[15] H. Schaller, G. Kaindl, F. Wagner, and P. Kienle, Phys. Letters **24B**, 347 (1967).

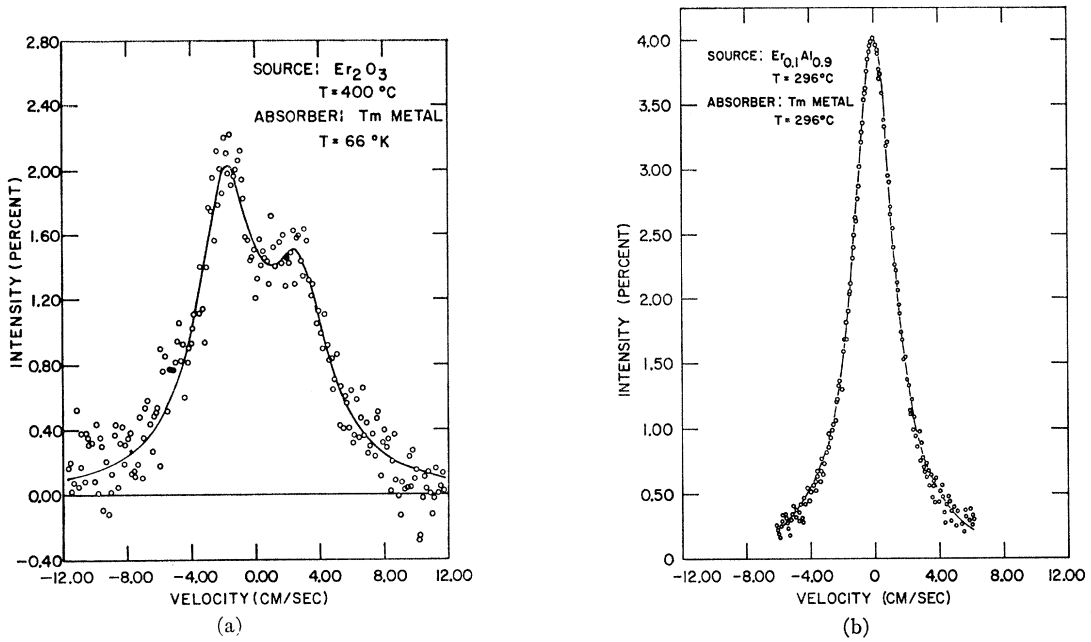

FIG. 2. Mössbauer-effect spectrum of Tm metal at (a) 66°K and (b) room temperature. For (a) the solid line is the best fit of two Lorentzian line shapes to the data points. For (b) the solid line is the best fit of one Lorentzian line shape to the data.

the geometric curvature (to a first approximation), the two halves of the data were folded over and summed. The channel address was then converted to velocity units and a function, which consisted of one Lorentzian line or the sum of two Lorentzian lines each multiplied by the background count, was fitted to the data using a χ^2 minimization procedure developed by Davidon [Figs. 2(a) and 2(b)].[16] In this fitting procedure the position, width, and intensity of each of the two lines as well as the background count could be treated as parameters. Because of the relatively poor resolution, however, the widths of the lines were constrained to be equal. When a minimum in the value of the function was located, several random steps were taken in an effort to determine whether a relative or an actual minimum had been located.

The final step in the analysis was to fit Eq. (14) to the measured temperature dependence, also by using the Davidon minimization procedure. The desired crystal potential parameters as well as the parameters ρ_1 and ρ_2' were determined by this final fitting.

Initial estimates for the crystal potential parameters had to be provided as a starting point for this minimization routine. The parameters required for D_{6h} symmetry are C_2^0, C_4^0, C_6^0, and C_6^6. The lattice-field gradient $q_{zz}^{(\mathrm{lat})}$, calculated using the planewise summation method of de Wette,[17] was used to determine A_2^0 from the relationship defined by Eq. (7). The unshielded parameter $A_2^0\langle r^2\rangle_{4f}$ was then evaluated using the value for $\langle r^2\rangle_{4f}$ of 0.19×10^{-16} cm^2, given by Judd and Lindgren.[18] Lattice-sum calculations provided the ratio A_4^0/A_6^0 which, with the values for $\langle r^4\rangle_{4f}$ of 0.069×10^{-32} cm^4 and for $\langle r^6\rangle_{4f}$ of 0.037×10^{-48} cm^6 given by Judd and Lindgren,[18] was used to evaluate the ratio C_4^0/C_6^0. The ratio C_6^6/C_6^0 was obtained by using the ordinary lattice sums. Since these sums converge very rapidly for $n>2$, only the first 92 neighbors in thulium metal were included. An upper limit on the ionic energy-level separation was set by observing the temperature at which the quadrupole interaction leveled out. Using second-order perturbation theoretic expressions for the energy levels, an estimate of the value of C_6^0 was made. From this value, estimates for all the other crystal-field parameters were made using the ratios mentioned above. Estimates for ρ_1 and ρ_2' were made using the high- and low-temperature limits of the quadrupole splitting, respectively, i.e.,

$$(\Delta E)_T = 2C_2^0\rho_2', \qquad T>160^\circ\mathrm{K}, \tag{15}$$

$$(\Delta E)_T = \tfrac{1}{2}(C_2^0\rho_1\langle 1 \mid 3J_z^2 - J^2 \mid 1\rangle + 4C_2^0\rho_2'), \qquad T\sim 0^\circ\mathrm{K}, \tag{16}$$

where the average, $\langle 1 \mid 3J_z^2 - J^2 \mid 1\rangle$, is the contribution to the field gradient of the lowest-lying energy level. In cases where there are two low-lying levels, this average is replaced by the contribution of both levels. The computer fitting program used these estimates as starting values in the minimization routine.

The eigenvalue problem for the Hamiltonian given by Eq. (4) was solved in the fitting routine. This was

[16] W. C. Davidon, Argonne National Laboratory Report No. ANL-5990 Rev., 1959 (unpublished).
[17] F. W. de Wette, Phys. Rev. **123**, 103 (1961).
[18] B. R. Judd and I. Lindgren, Phys. Rev. **122**, 1802 (1961).

TABLE II. A comparison of the resulting sets of CEF parameters obtained by using different sets of initial guesses. The values of the C_n^m obtained in the manner discussed in Sec. IV are $C_2^0=-106.2$, $C_4^0=-9.0$, $C_6^0=+2.5$, and $C_6^6=-26.6$.

	C_2^0 (cm^{-1})	C_4^0, C_6^0, C_6^6 (cm^{-1})	ρ_1 (10^{-5})	ρ_2' (10^{-5})	Δ (cm^{-1})	R_Q	σ_2
1[a]	−69.7	0.0 0.0 0.0	−1.62	2.25	76.1	0.16	0.34
2[b]	−66.5	−8.3 2.3 −26.3	−1.58	2.27	79.9	0.22	0.37
3[c]	−77.2	8.0 −2.3 26.2	−1.62	2.59	77.2	0.07	0.27
4[d]	48.0	−10.6 2.0 −27.4	−4.65	−4.47	45.8	2.67	1.45

[a] C_4^0, C_6^0, and C_6^6 were constrained to equal zero.
[b] The initial parameter estimates obtained via the method of Sec. IV were used. (Data of Ref. 7.)
[c] The same initial estimates used in b were used except that the signs of C_4^0, C_6^0, and C_6^6 were changed.
[d] The same initial estimates used in b were used except that the sign of C_2^0 was changed.

necessary in order to determine the contribution of each ionic level to the field gradient. The final solution thus includes the ionic energy-level spacings and the associated wave functions.

V. RESULTS

As was pointed out in Sec. II, the appropriate lattice sums were carried out in order that initial estimates of the CEF parameters could be made. It was found, however, that the fitting routine was sensitive only to C_2^0, ρ_1, and ρ_2' (see Table II). The parameters C_4^0, C_6^0, and C_6^6 were constrained to be zero, and the resulting fit of theory to experiment (Fig. 3) was as good as when the above-mentioned initial estimates

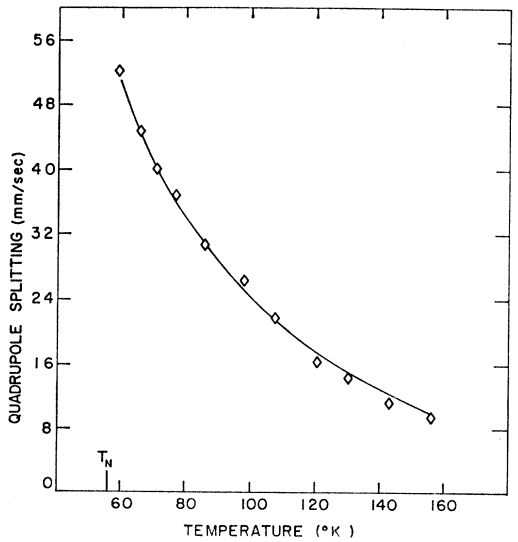

FIG. 3. Temperature dependence of the quadrupole splitting of the 8.42-keV excited state of Tm^{169} in thulium metal. The solid line is the best fit of Eq. (14) in the text to the data. This fit was obtained for the constraining conditions that C_4^0, C_6^0, and C_6^6 equal zero. The resulting values of the remaining parameters are given in line 1 of Table II.

of these latter parameters were used. In fact, the signs of these three parameters could be changed from the initial estimates without affecting the resulting fit or appreciably altering the values of C_2^0, ρ_1, and ρ_2', and the over-all splitting Δ of the ground term. In all cases, the average deviation between the fitted function and the experimental curve was less than the experimental uncertainty in the measurement of each individual datum.

An attempt to fit the data with a positive C_2^0 value rather than with a negative value (as determined from the de Wette calculation) was also successful. The resulting values of R_Q and σ_2, however, contradict existing theory.[11] As is shown in Table II, the values of R_Q and σ_2 which were obtained from Eqs. (6) and (12) by using the positive C_2^0 and the corresponding ρ_1 value are completely inconsistent with present theoretical calculations. In contrast, all the sets of R_Q and σ_2 values obtained with negative C_2^0 are in reasonably good agreement with theoretical expectations,[11] independent of the values of C_4^0, C_6^0, and C_6^6 which are involved.

Contrary to what is found to be the case for thulium ethyl sulfate (TmES), where the magnitudes of C_4^0 and C_6^0 are substantial fractions of C_2^0 and C_6^6 is roughly three times larger than C_2^0, these calculated parameters for the metal are considerably smaller fractions of C_2^0 (see Table II). This, then, accounts for the fact that these parameters cannot be neglected in fitting theory to experiment in the case of TmES, whereas they are essentially negligible in the metal.

The final fit of theory to the experimental data points is shown in Fig. 3. The parameters C_4^0, C_6^0, and C_6^6 were constrained to be zero, and the resulting values of C_2^0, ρ_1 and ρ_2', and Δ are tabulated on line 1 of Table II. These values will be used in all further calculations and discussion. The associated ionic energy levels and wave functions are listed in Table III.

TABLE III. Ionic energy levels and associated wave functions for thulium metal.

Energy (cm^{-1})	Degeneracy	Wave function	$\langle 3J_z^2-J^2\rangle$
0.0	2	$\|\pm6\rangle$	66
23.3	2	$\|\pm5\rangle$	33
42.3	2	$\|\pm4\rangle$	6
57.0	2	$\|\pm3\rangle$	−15
67.6	2	$\|\pm2\rangle$	−30
74.0	2	$\|\pm1\rangle$	−39
76.1	1	$\|0\rangle$	−42

VI. DISCUSSION

A. CEF Effects

The main purpose of this study was to investigate crystal electric field effects in metallic thulium. The investigation was carried out in the paramagnetic regime at temperatures above the magnetic ordering temperature. This was done in order to study the CEF effects directly. Thus, complications due to magnetic-exchange interactions, for example, do not arise.

Generally speaking, one expects that the present measurements on thulium metal should be more readily interpretable than those made, for example, on intermetallic compounds of thulium. In particular, the intermetallics are complicated by the presence of a second metal ion which makes the assignment of the effective valences of the ions difficult and introduces considerable uncertainty into the lattice-sum calculations. On the other hand, in the case of the pure metal (thulium), the signs of the lattice-sum calculations must be correct. Even though the Tm^{3+} ions may be screened by local distribution of conduction electrons, the sign of the charge which enters the lattice-sum calculations will always be positive. The signs of the calculated lattice sums should therefore be correct, though the magnitudes will depend on the degree of screening which is assumed.

Elliott[2] has calculated values of the lattice sums for the hexagonal rare-earth metals, assuming that the nearest neighbors are tri-positive and that the remainder of the lattice is neutral, being screened by the conduction electrons. Combining the values obtained for $\langle r^n\rangle_{4f}$ by Judd and Lindgren[18] with Elliott's sums yields the CEF parameter values for thulium which are listed in column 1 of Table IV. To be compared with these are the values (column 2 of Table IV) obtained assuming no screening at all. The de Wette method was used to calculate C_2^0, and the other parameters are based on direct lattice sums over the first 92 neighbors of the central ion. In both cases, the magnitudes of C_4^0, C_6^0, and C_6^6 are small compared to the magnitude of C_2^0. This reinforces the hypothesis that these parameters do not play a significant role in splitting and mixing the zero-order states of the $(4f)^{12}$ ground term. It seems reasonable, therefore, that the zero-order fit of theory to experiment (see Fig. 3 and Table II) obtained by constraining C_4^0, C_6^0, and C_6^6 to equal zero provides a close approximation to the real state of affairs.

The fact that Elliott's value for C_2^0 is closer to experiment than the de Wette value brings up the difficulty of just how to treat the conduction electrons. In this paper the non-s character of the itinerant electrons has been incorporated phenomenologically into a field-gradient term which adds onto the lattice contribution and appears in the definition of ρ_2'. Their screening effect on the Tm^{+3} ions in the lattice sums as was included by Elliott has not been included here. This is undoubtedly not completely correct since there is probably some screening. There are, however, two independent factors which tend to reduce the magnitude of C_2^0 as calculated via de Wette's method. They are: (1) the above-mentioned screening of the lattice ions, and (2) the shielding of the $4f$ shell from the lattice by the closed $(5s)^2$ and $(6p)^6$ shells. The latter is taken into account in Eq. (6) by σ_2. The latest calculation by Sternheimer gave $\sigma_2=0.48$ for thulium.[11] Accounting for the reduction of the de Wette C_2^0 value by σ_2 alone yields $\sigma_2=0.34$. To include the conduction-electron screening as indicated by Elliott would widen the gulf between theory and experiment considerably. For example, using Elliot's value for $A_2^0\langle r^2\rangle_{4f}$ yields $\sigma_2=-0.22$, which is unexplainable via the present theory. It is on this basis, therefore, that we have chosen to recognize the explicit effect of the conduction electrons only by the $q_{zz}^{(ce)}$ which appears in ρ_2'.

Using $\sigma_2=0.34$ along with our values for C_2^0, and ρ_2' (line 1 of Table II) and $Q=1.5b$, Sternheimer's value of $\gamma_\infty=-75.3$, and $\langle r^2\rangle_{4f}=0.19\times10^{-16}$ cm^2 as determined by Judd and Lindgren,[18] we find from Eq. (13) that $q_{zz}^{(ce)}=2.14\times10^{24}$ cm^{-3} which is of the same sign and larger in magnitude than the direct lattice contri-

TABLE IV. Comparison of CEF parameters calculated using Elliott's sums for the case of extreme screening and those calculated in this work for the case of no screening of the Tm^{+3} ions by the conduction electrons.

Parameters	Elliott (1st neighbors $z=3$) (cm^{-1})	Lattice sums (92 nearest neighbors with $z=3$) (cm^{-1})
$A_2^0\langle r^2\rangle_{4f}$	−57.0	−106.2 (de Wette)
$A_4^0\langle r^4\rangle_{4f}$	−4.1	−1.9
$A_6^0\langle r^6\rangle_{4f}$	+0.6	+0.5
$A_6^6\langle r^6\rangle_{4f}$	−3.3	−5.6

where: a=3.5375 Å, c=5.5546 Å, $\langle r^2\rangle_{4f}=0.19\times10^{-16}$ cm^2, $\langle r^4\rangle_{4f}=0.069\times10^{-32}$ cm^4, $\langle r^6\rangle_{4f}=0.037\times10^{-48}$ cm^6.

bution given by

$$q_{zz}^{(\mathrm{lat})} = -4C_2^0(1-\gamma_\infty)/e^2(1-\sigma_2)\langle r^2\rangle_{4f} = 1.45\times10^{24}\ \mathrm{cm}^{-3}. \quad (17)$$

Here, the lattice contribution differs from Eq. (7) because it is multiplied by $(1-\gamma_\infty)$ for direct comparison at the nucleus.

The atomic shielding factor R_Q can be determined from the value obtained for ρ_1. Using ρ_1 and C_2^0 from line 1 of Table II, $Q=1.5b$, and $\langle r^{-3}\rangle_{4f}=75.5\times10^{24}$ cm^{-3} as found by Lindgren,[19] results in $R_Q=0.16$. This is in surprisingly good agreement with theory (Table II) inasmuch as the theoretical calculations are so difficult.

B. Comparison with Ferromagnetic State

Since the ground state of the split $^3H_6$ ground term (Table IV) is effectively the ferromagnetic state, the expected quadrupole splitting when only this state is populated ($T=0$, assuming that Tm does not order magnetically) should be identical to the measured splitting in ferromagnetic thulium metal. Kalvius *et al.*[6] have found that the splitting (Δv) in ferromagnetic thulium ($T=5$°K) is 14.6 cm/sec. This agrees very well with $\Delta v=15.1$ cm/sec obtained by substituting our results into Eq. (16) which gives the expected splitting at $T=0$°K, assuming that thulium does not order magnetically and is described by the states given in Table III.

For temperatures large compared to Δ, Eq. (15) yields $\Delta v=-1.4$ cm/sec. This is similar to the results obtained for Tm_2O_3[1] and indicates that with better resolution than was attained in the present work, it may be possible to observe the quadrupole splitting vanish when the contributions of opposite sign cancel.

C. Asymmetries and Low-Temperature Effects

As can be seen in Fig. 2, there is an asymmetry in the intensities of the two lines of the Mössbauer spectrum. Goldanskii *et al.*[20] were the first to provide a plausible explanation of this phenomenon. They pointed out that for crystal symmetries which are less than cubic, the recoil-free fraction may be anisotropic, i.e., the fact that the bonds which hold the atom in the lattice may be stronger in one crystalline direction than in another leads to an asymmetry in the intensities when averaged over all possible crystal orientations with respect to the direction of the incident γ beam. Since the absorbers used in the present experiments were rolled foils, the possibility of "rolling in" a preferred direction would enhance any anisotropy due to an anisotropic recoilless fraction.

A second possible cause of the anisotropy is the presence of spin-lattice relaxation effects. For example, if the spin-lattice relaxation time for the $4f$ electrons is longer than the time characteristic of the magnetic interaction between the nuclear spin moment and the $4f$-electron moment, then the nucleus will experience a net nonzero magnetic hyperfine field. The magnitude of such an interaction will be larger for the $M_I=\pm\frac{3}{2}$ level than for the $M_I=\pm\frac{1}{2}$ level, thereby leading to an anisotropy of the linewidths.[21] That such a situation could exist in thulium metal in the presence of the *s-f* spin-lattice relaxation mechanism, is, however, difficult to imagine, especially at temperatures above 59°K.

Also noted in the spectra was a pronounced line-broadening (25%) as the temperature decreased from 100 to 59°K. Since the broadening occurred well above the ordering temperature, it could not be attributed to the exchange interaction. Experimental effects (e.g., instrumentation) were ruled out because the splitting of Tm_2O_3 was observed at 4.2°K using the maximum velocity of the system, and this spectrum showed no observable broadening.

A tempting explanation for this broadening is that the crystal-field potential is not completely homogeneous. That is, instead of having a unique value as has been assumed, the CEF may vary in a random manner throughout the lattice. Impurities, strains, and other imperfections could give rise to such variations. Such imperfections are common in metals but can often be removed by suitable annealing treatment. Line broadening in the nuclear-magnetic-resonance spectra of certain hexagonal metals has been accounted for in a similar manner,[22] and in fact, this is probably why nuclear magnetic resonance has not been observed in some metals (e.g., titanium and zirconium).

Unfortunately, the rather high vapor pressure of thulium makes it difficult to anneal at what would be the ideal temperature. Consequently, even though the metal was annealed at 775°C for 2 h, the temperature-dependent broadening remained. On this basis, we are not able to conclude whether or not the broadening is due to a distribution of CEF values or to relaxation effects which might also lead to this behavior.

ACKNOWLEDGMENTS

The authors are indebted to Dr. F. H. Spedding for making available the rare-earth metals used in this investigation. The Er-Al alloys used for the sources were prepared by B. J. Beaudry, and the foils were prepared by L. K. Reed and G. L. Ahrens. The assistance of Dr. R. A. Reese and Dr. D. J. Genin with instrumentation and computer programming is gratefully acknowledged.

[19] I. Lindgren, Nucl. Phys. **32**, 151 (1962).
[20] V. I. Goldonskii, E. F. Makarov, and V. V. Krapov, Phys. Letters **13**, 344 (1963).
[21] M. Blume, Phys. Rev. Letters **14**, 96 (1965); E. Bradford and W. Marshall, Proc. Phys. Soc. (London) **87**, 731 (1966).
[22] B. R. McCart and R. G. Barnes, Bull. Am. Phys. Soc. **12**, 315 (1967).